Proceedings of the ASME 2023
International Mechanical Engineering Congress and Exposition
IMECE2023
October 29–November 2, 2023, New Orleans, LA

IMECE2023-113489

EXPERIMENTAL IDENTIFICATION OF REDUCED ORDER MODEL PARAMETERS FOR HYDROKINETIC ENERGY SYSTEM DESIGN

Austin L. Griffin[1], Yong Hoon Lee[1,*]

[1]Department of Mechanical Engineering,
The University of Memphis, Memphis, TN

ABSTRACT

This study presents the ongoing development of experimental validation and identification of the reduced order model (ROM) parameters for the horizontal axis hydrokinetic turbine (HAHkT) in the context of design optimization. It is crucial to optimize the HAHkT scale, external and internal geometry, rotor and blade design, and control scheme simultaneously to achieve cost-efficient energy conversion. However, high-fidelity simulation models, such as three-dimensional computational fluid dynamics (CFD), are costly, making the ROM approach more practical in the optimization loop. Based on the existing circuit analogy ROM model for the ducted HAHkT, we focus on improving the model by incorporating previously ignored model parameters, such as turbine rotor resistance, to enhance the fidelity of the ROM. We use turbine blade hydrodynamic simulation results based on blade element momentum (BEM) theory to augment the ROM fidelity. The open channel experiment will test various geometries and blade pitches to validate and identify fine tuning parameters of the developed ROM. Additive manufacturing will be used to fabricate turbine components and ducts. Pressure, water velocity, turbine rotational speed, and torque on the shaft will be collected. The improved ROM, validated through experiments and simulations, can be used for a broader range of designs, contributing to the development of a cost-efficient HAHkT system for renewable energy system designers.

Keywords: Reduced Order Model (ROM), Hydrokinetic Turbine (HkT), Horizontal Axis Hydrokinetic Turbine (HAHkT), Open Channel Water Flume

1. INTRODUCTION

As the world population continues to grows exponentially, so too does the demand for energy [1, 2]. The global use of fossil fuels for energy production has been clearly linked to negative impacts on the climate [3]. In recent years, there has been a significant increase in research surrounding the development and utilization of renewable energy sources, such as hydrokinetic turbines (HkTs), as a means to mitigate climate change [4, 5]. Horizontal-axis hydrokinetic turbines (HAHkTs) have gained considerable attention due to the benefits of lower start-up current speed and higher output than vertical-axis turbines [6, 7]. To achieve cost-efficient energy conversion, it is crucial to optimize the HAHkT scale, external and internal geometry, rotor and blade design, and control scheme simultaneously, which requires a holistic design approach known as the control co-design (CCD) method [8, 9].

However, designing these systems presents challenges, primarily due to the lack of validated simple models that can be used in system-level optimization problems. Many models used for design optimization of HAHkTs are based on high-fidelity computational fluid dynamics (CFD) models, which are generally computationally-expensive [10, 11], or reduced order models (ROMs), which are mostly limited to certain flow conditions [12]. HAHkT models based on CFD are generally impractical for dynamic system design optimization with CCD, due to the high dimensionality of the design optimization problem, demanding excessive number of expensive function evaluations. Therefore, the reduced order model (ROM) approach has gained substantial attention as an efficient tool for designing complex renewable energy systems, including HAHkT systems [12, 13].

The ROM approach involves developing a simplified mathematical model that captures the essential dynamics of the system while reducing the computational cost significantly. In previous literature, electrical circuit analogy numerical models have shown great potential as ROM representations of ducted HAHkT systems [12]. This previous model has been simulated at contraction ratios of 1, 1.33, and 2. The results displayed duct entrance to throat velocity ratios of 1, 2, and 4 respectively which corresponds with the continuity of flow as area changes. Ducted HAHkTs, in particular, show promise for future use as the duct significantly increases power and can be used in a modular setting [11, 12, 14, 15]. In addition, it has been found that the average

*Corresponding author: yhlee@memphis.edu

Copyright © 2023 by ASME

wind flow speed increased up to 1.75 times the free stream velocity [16]. The speed increase also applies to water, and the increased flow speed for the HkT system is more impactful because the energy density of water is significantly higher than wind [7].

The ROM approach proposed in Bilgen et al. [12] is a highly efficient circuit analogy model that is particularly suitable for optimizing expensive CCD problems. However, the model does not take into account the effects of turbine blades, which can lead to inaccurate design results when blades are present. To enhance the fidelity of the circuit analogy ROM for detailed design of HAHkT systems, this study aims to develop an experimental setup to validate, improve, and tune the circuit analogy ROM by identifying and incorporating model parameters, which are ignored in previous literature. This new ROM will accurately account for the rotor resistance instead of assuming it as zero, thereby facilitating the use of a more precise model in HAHkT design. This will, in turn, enable the design of a system that considers the performance implications arising from changes in rotor design. Previous work predominantly focused on contraction ratio as the most interested parameter. The experimental work presented in this paper aims to uncover sensitivities in relation to both the contraction ratio and rotor resistance.

2. METHODS

This study consists of (1) the development of an enhanced ROM model that accounts for the turbine rotor in the ducted HAHkT system, (2) a simulation of the HAHkT rotor blades based on blade element momentum theory to augment the enhanced ROM, and (3) the development of an experimental setup for validating and tuning the developed model.

2.1 Enhanced Reduced Order Model

The circuit analogy model [12] employs the "mechanical" resistance for flow channel sections inside and outside of the duct, expressed in Ohm's law, given as:

$$R = \frac{\Delta V}{I} = \frac{\Delta p}{Q}, \tag{1}$$

where R is the resistance of each section in the flow path. V and I are voltage and current in the electrical circuit, analogous to pressure p and flow rate Q, respectively in the fluid flow circuit. This previous model makes several assumptions for simplification, including laminar, incompressible, and steady flow conditions [12]. The most notable assumption is that the rotor resistance equates to zero. Figure 1 illustrates an updated control volume with resistances represented for each segment. With the given analogy, the equivalent resistance for the rotor can be found with:

$$R_{\text{rotor}} = \frac{p_2 - p_3}{Q_{\text{duct}}}, \tag{2}$$

where R_{rotor} is rotor resistance, p_2 is the pressure before the rotor blades, and p_3 is the pressure after the rotor blades. Bernoulli's equation must be used to determine p_2, given as:

$$p_2 = p_1 + \frac{1}{2}\rho\left(\left(\frac{Q_{\text{duct}}}{A_1}\right)^2 - \left(\frac{Q_{\text{duct}}}{A_2}\right)^2\right) - \Delta p_{12}, \tag{3}$$

where p_1 is the pressure at the duct inlet, ρ is water density, and Q_{duct} is the flow rate for the duct. The pressure after the rotor is then determined by the following relation:

$$p_3 = \frac{P_{\text{available}} - P_{\text{extracted}}}{Q_{\text{duct}}} - \frac{1}{2}\rho v_2^2. \tag{4}$$

The power extracted by the rotor, $P_{\text{extracted}}$, and power available right before the rotor, $P_{\text{available}}$ will be determined theoretically and experimentally. With R_{rotor} found and integrated into the existing framework, the new ROM will have enhanced fidelity for use in accurate design optimization.

2.2 Blade Element Momentum Simulation

HAHkT blade element momentum (BEM) simulations are performed in QBlade to analyze the blades of a turbine [17]. QBlade developed by TU Berlin, models a rotor blade with a specific airfoil distributed over different radial sections of the blade [18]. The turbine local blade forces, with a momentum balance over the rotor disc models the flow field [18]. QBlade was originally intended for wind turbines; however, it is shown that general purpose aerodynamic and aero-elastic simulation tools for wind turbines can be utilized for the design of HAHkTs [19]. QBlade offers a user-friendly, visual interface, featuring essential functions that must be executed before performing BEM simulations. These functions encompass performing an Xfoil analysis and a 360-degree (°) extrapolation of this analysis for a given Reynolds number and airfoil geometry [17]. Xfoil is a linear vorticity stream function panel method which includes a viscous solution which interacts with the incompressible potential flow via a surface transpiration model [20]. The Xfoil analysis yields lift coefficients, drag coefficients, moment coefficients, pressure distributions, velocity distributions, glide ratios, and boundary layers for a specific airfoil geometry and Reynolds number over various angles of attack. This Xfoil data is then extrapolated to encompass all 360° of angle of attack, which is used to create an overall airfoil Reynolds profile file. QBlade utilizes data provided from the Xfoil analyses to extrapolate 360° polar data. This extrapolated data and user-defined parameter inputs are used to perform the simulation. Torque and power coefficient data are collected from simulations performed where tip speed ratio and pitch are varied. QBlade does not allow for duct inputs, but is still essential for understanding the rotor behavior in a free stream where the velocity could be equivalent to that of a ducted rotor. The power coefficient for a particular turbine is determined with the expression:

$$C_P^* = \left(\frac{P_{\text{extracted}}}{P_{\text{available}}}\right). \tag{5}$$

This power coefficient utilizes the free stream velocity and the rotor area, producing a power coefficient that abides by the Betz limit of 0.593 [19]. This power coefficient can be corrected, with respect to the entire turbine duct, by the following expression [11]:

$$C_P = C_P^*\left(\frac{A_{\text{exit}}}{A_{\text{rotor}}}\right). \tag{6}$$

The power available for the fluid is then determined to be [12]:

$$P_{\text{available}} = \frac{1}{2}\rho A_2 v_2^3, \tag{7}$$

Copyright © 2023 by ASME

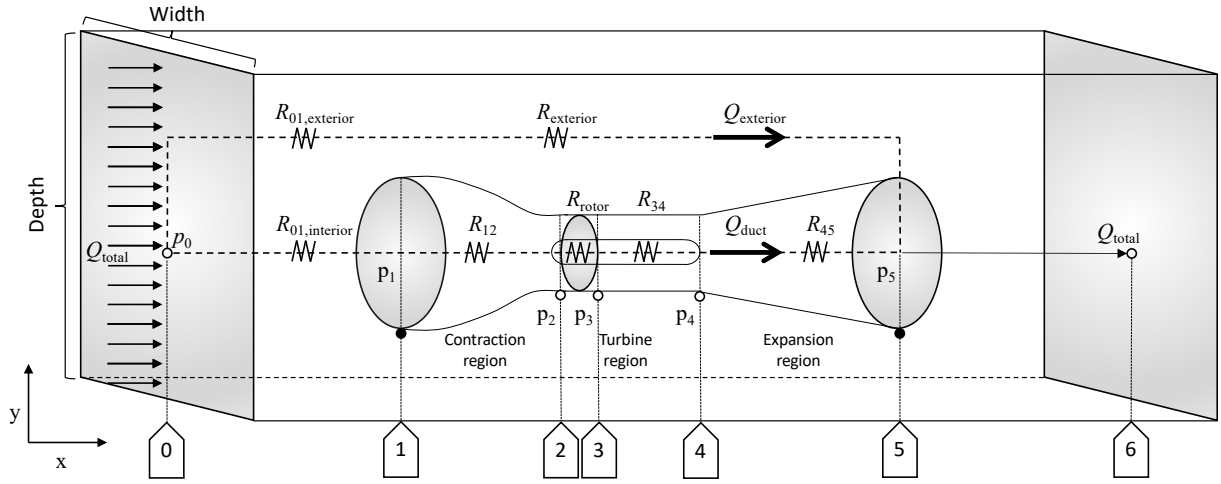

FIGURE 1: CIRCUIT ANALOGY ROM OF THE HAHKT ENHANCED FROM MODEL PRESENTED IN REF. [12]

FIGURE 2: OPEN CHANNEL FLUME

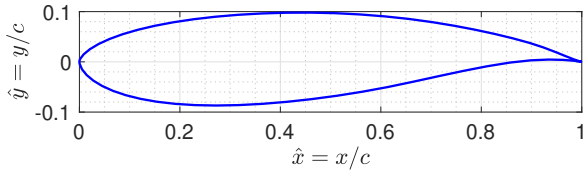

FIGURE 3: NORMALIZED PROFILE OF NREL S833 HYDROFOIL

where A_2 is the area at the duct throat. With the power available and the power coefficient, the power extracted can be solved for. With the power available and the power extracted, the pressure after the rotor, p_3, can be solved. Finally with the pressure known before and after the rotor, the equivalent resistance of the rotor can be determined with Eqns. (2) and (3).

2.3 Design of Experimental Setup

This experimental work utilizes an open channel flume shown in Fig. 2 to create controlled water flow in the axial direction of the HAHkT apparatus. The open channel is 4.42 meters long and will be modified to include a 1.5 m insert where the cross-sectional area is reduced to 240 mm by 240 mm which is intended to increase the initial average velocity of 0.1 m/s. A converging-diverging duct is installed to increase the flow velocity at the turbine region. To maximize the flow from the decreased area to the a given duct without any exterior flow around the duct entrance, an even larger funnel is installed for each duct entrance. This maximized flow gives a Reynolds number of 61,500 at the tip of the blade. We assume that the water flow is incompressible and reside within the transitional regime, owing to the anticipated range of Reynolds numbers. While flow separation could potentially be observed at higher angle of attack, our operational range avoids the stall regime of the blade profile. The temperature of

Copyright © 2023 by ASME

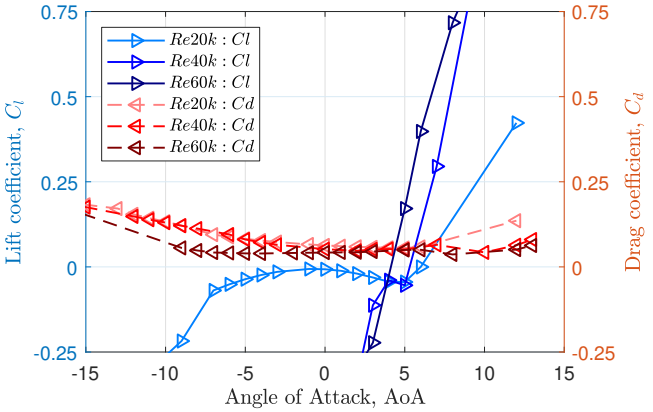

FIGURE 4: LIFT AND DRAG COEFFICIENTS AS FUNCTIONS OF ANGLE OF ATTACK AT VARIOUS REYNOLDS NUMBERS

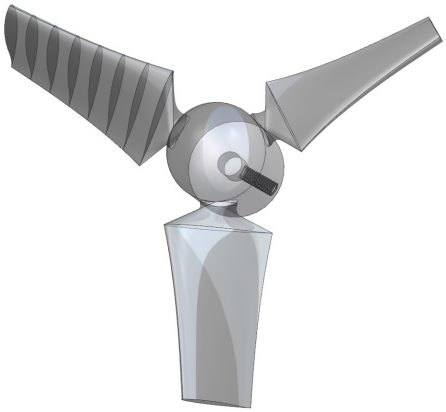

FIGURE 5: FRONT VIEW OF THREE-DIMENSIONAL MODEL FOR ROTOR MODEL

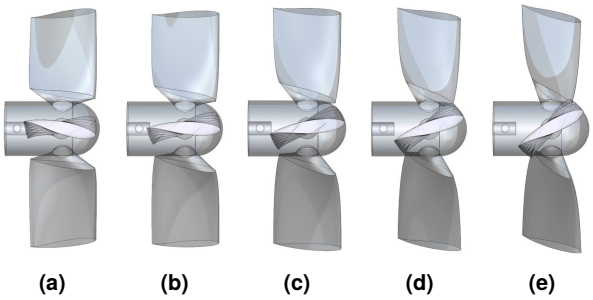

FIGURE 6: THREE-DIMENSIONAL ROTOR MODELS WITH VARIED BLADE CONTROLLED PITCH

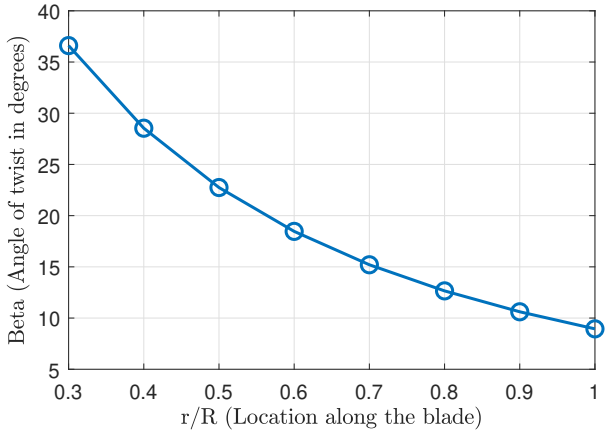

FIGURE 7: ANGLE OF TWIST DESIGNED AS A FUNCTION OF NORMALIZED RADIUS ALONG THE BLADE

the flow is considered to be a constant 20°C. In large deep sea application, temperature gradients may lead to thermal stratification, though not explored in this paper, may have a substantial effect on the stability of turbine wakes, which is necessary to understand for efficient deep water turbine farm arrays [21].

The design of a small-scale HAHkT in an open channel flume comprises various components that must be printed, constructed, or procured. The actual design will consist of the following: a rotor assembly where blades can be replaced and pitch can be altered, an enclosed shaft leading into a 90° bevel gear, another enclosed shaft inline with a brushed DC motor acting as a generator with voltage and amperage measured, a tachometer to measure the shaft rotational speed, and a modular duct surrounding the turbine. The blade geometries chosen to assess come from NACA, NREL, and Eppler, all of which have shown promising results when used as hydrofoils [22, 23].

The selected blade profile, NREL S833, is displayed in Fig. 3. In order to find a suitable inital α, angle of attack, XFOIL analyses were performed in QBlade from $-15°$ to $+15°$ with a Reynold's numbers representing the root of the blade, the mid section of the blade, and the tip of the blade. The corresponding Reynold's numbers were rounded to the nearest 10,000 to produce 20,000, 40,000, and 60,000 respectively. The results for these analyses are shown in Fig. 4. From this figure it can be seen that certain points were not recorded due to stall. Previous work at higher Reynold's numbers came to a conclusion that 6° is the ideal α [24]. However, in the figure it can be noted that the drag coefficient overtakes the lift coefficient at 6° for a Reynold's number of 20,000 and therefore should be excluded. With this mind the α of 7° was chosen as a baseline angle of attack (α_0) for expected Reynold's number range. Figure 5 displays the front of the rotor hub apparatus slightly offset. Figure 6 displays a side view of the rotor hub apparatus as pitch was varied from $-20°$ to $+20°$ in increments of 10°. The appropriate angle of twist, β is displayed in Fig. 7. β for the blade sections was calculated with the following relationship:

$$\beta = \tan^{-1}\left(\frac{U}{r\omega}\right) - \alpha_0, \tag{8}$$

where U is the nominal velocity, which was set to 0.678 m/s, ω is the nominal rotational speed, which is set to 30.5 rad/s, and r is the distance along blade which began at a radius of 15 mm and increased by increments of 5 mm till the tip at 50 mm. This ensures that all local blade section locations have baseline angle of attack at the nominal flow speed and optimal TSR, when controlled blade pitch (θ_p) is maintained at 0°. Figure 7 displays the change in β along the length of the blade. U and ω were chosen as such to produce a tip speed ratio, TSR, of 2.25 with the

Copyright © 2023 by ASME

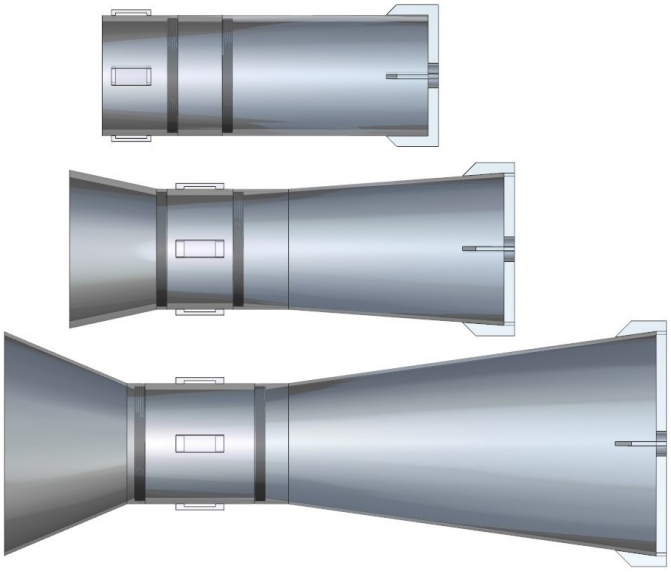

FIGURE 8: DUCT CONFIGURATIONS WITH INLET/OUTLET DIAMETERS OF 104, 138, AND 208

following relationship:

$$\text{TSR} = \left(\frac{r\omega}{U}\right), \tag{9}$$

Chord length was kept constant along the blade for experimental simplicity. Change in chord, tip clearance, and cavitation were not explored but are essential to incorporate for full CCD optimization. In total, nine different rotor designs with each at a different fixed pitch, as well as other components, will be printed in the additive manufacturing lab at the University of Memphis which employs a binder jetting process for metal printing. The modular ducts, which will allow for easy adjustments to the divergent and convergent ends, will be printed in the polymer PETG via an extrusion process using a Creality CR-M4 printer. Figure 8 display the designs for each of the ducted assemblies to be printed and tested.

Lastly, the flow generated from the pumps is constant and therefore the flow is assumed to be steady. The primary objective for the experiment is to collect rotational speed, voltage, amperage, and torque data for various duct geometries and blade pitches. The free stream flow will also be assessed with a flow meter. This collection of data will be essential in formulating the experimental power coefficient with the following relationship:

$$C_P^{**} = \left(\frac{M\omega}{\frac{1}{2}\rho A v^3}\right). \tag{10}$$

Thereafter, determining the experimental rotor resistance with using C_P^{**}, Eqns. (2), and (3). These results will also be compared to the simulated results and validity will be determined for the enhanced ROM. The C_P^{**} can also be corrected to find the power coefficient value associated with the entire duct, which abides by the Betz limit, using the following relationship:

$$C_P^{*} = C_P^{**}\left(\frac{A_{\text{rotor}}}{A_{\text{exit}}}\right). \tag{11}$$

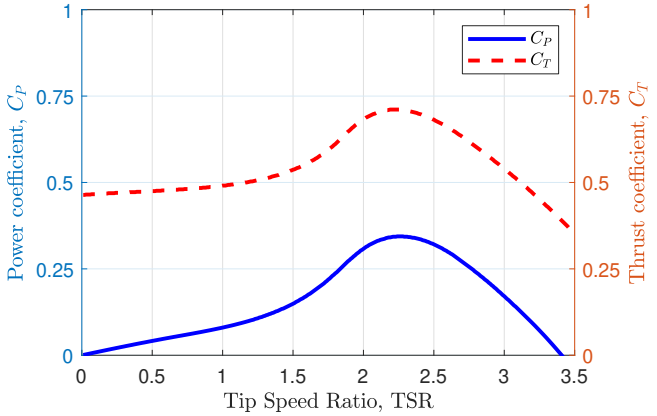

FIGURE 9: POWER AND THRUST COEFFICIENTS AS A FUNCTION OF TSR

2.4 Design Optimization Plans

Dynamic system design optimization plans employing CCD methodology for a reduced order model of ducted HAHkTs will lead to substantial advancements in performance and efficiency. By concurrently addressing physical and control system design problems, the CCD approach can effectively tackle complex interactions and trade-offs in the design process, resulting in system-optimal design solutions. This methodology will facilitate the development of advanced ducted HAHkTs, fostering renewable energy adoption and environmental sustainability. With the developed ROM, which accounts for the turbine rotor and blade effects through numerical and experimental parameter identification, design engineers and researchers will be able to optimize with a wide range of design options to develop novel turbines with higher efficiency, utilizing both physical design and novel control strategies. The enhanced ROM will provide a readily available model that can be easily integrated into the CCD optimization loop, applicable to a variety of hydrokinetic energy applications, thereby further enhancing the performance and resilience of these systems. The incorporation of this ROM into the CCD optimization loop allows for more comprehensive multidisciplinary considerations in the design processes, especially when the design problem involves active dynamic controls of the HAHkT in various design load case scenarios.

3. PRELIMINARY RESULTS

A QBlade simulation was conducted to generate power and thrust coefficient data for various TSRs, ranging from 0.1 to 3.5. The inputs for the blades were the same as the experimental inputs, with the blade profile of NREL S833 selected and the angle of twist varied following local speed ration, as shown in Fig. 7. Figures 9 and 10 present these results for the simulations where tip speed ratio and pitch were each varied respectively. Figure 11 presents the results for coefficient of power varying pitch at multiple tip speed ratios. Based on these figures, the maximum power coefficient can be determined and corrected with Eqn. (6). The power available is then calculated with Eqn. (7). With the power coefficient and the power available, the power extracted can be computed. With the power available and the power extracted, using Eqn. (4), the pressure after the rotor is determined. Finally

Copyright © 2023 by ASME

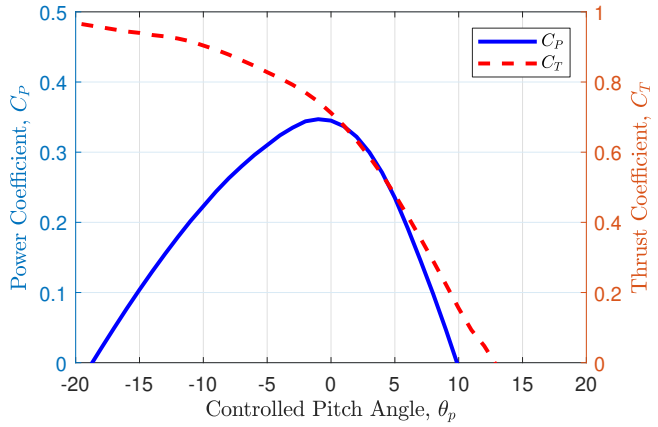

FIGURE 10: POWER AND THRUST COEFFICIENTS AS A FUNCTION OF PITCH AT 2.25 TSR

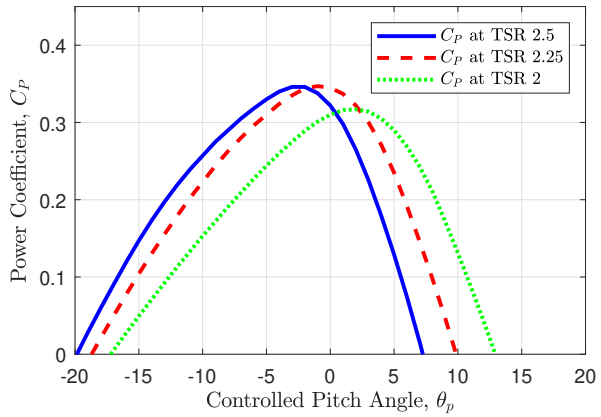

FIGURE 11: POWER AND THRUST COEFFICIENTS AS A FUNCTION OF PITCH AT VARYING TSR

with the the pressure before the rotor calculated from Eqn. (3), and the pressure after the rotor known, the equivalent rotor resistance can be calculated with Eqn. (2).

In the final version of the paper, we will present a comprehensive experimental design and setup, outlining detailed plans for connecting the enhanced ROM parameters with the measurements obtainable through the experiment. This approach will enable a more accurate representation of the system, allowing for better optimization and performance evaluation of ducted HAHkT systems.

4. CONCLUSION

In conclusion, integrating power coefficient results from simulations and experiments into the calculation of equivalent resistances for rotor blades significantly enhances the existing one-dimensional ROM, which previously omitted these essential turbine rotor elements. Although slightly more complex due to the inclusion of rotor blade resistance, the improved ROM provides a more accurate representation of the resistance distribution along a ducted HAHkT and offers a critical avenue for incorporating CCD.

The primary expected contribution of this research to HAHkT design optimization and renewable energy system development lies in providing a more accurate and reliable model for designing and evaluating HAHkTs. By incorporating the rotor resistance, which can be easily calculated using a known power coefficient for a given turbine, this enhanced ROM facilitates a streamlined approach for one-dimensional HAHkT design optimization.

The potential benefits of the improved ROM for ocean renewable energy system designers are numerous. This enhanced model enables more efficient design iterations, reduces computational complexity, and allows for more accurate performance predictions. As a result, designers can optimize HAHkT configurations more effectively, contributing to the advancement of renewable energy systems and promoting more sustainable energy solutions.

This new ROM will be rigorously validated and refined through a series of experiments and simulations involving rotor blades with known power coefficients. This validation process will ensure the model's reliability and accuracy in predicting the performance of HAHkT systems, ultimately leading to more effective design optimization and renewable energy system development.

REFERENCES

[1] Olabi, A. G. and Abdelkareem, Mohammad A. "Renewable energy and climate change." *Renewable and Sustainable Energy Reviews* Vol. 158 (2022): p. 112111. DOI 10.1016/j.rser.2022.112111.

[2] Neha and Joon, Rambeer. "Renewable energy sources: A review." *Journal of Physics: Conference Series* Vol. 1979 (2021): p. 012023. DOI 10.1088/1742-6596/1979/1/012023.

[3] Soeder, Daniel J. "Fossil Fuels and Climate Change." *Fracking and the Environment: A scientific assessment of the environmental risks from hydraulic fracturing and fossil fuels* (2021): pp. 155–185.

[4] Saini, Gaurav and Saini, Rajeshwer P. "A review on technology, configurations, and performance of cross-flow hydrokinetic turbines." *International Journal of Energy Research* Vol. 43 No. 13 (2019): pp. 6639–6679. DOI 10.1002/er.4625.

[5] Sood, Manoj and Singal, Sunil K. "Development of hydrokinetic energy technology: A review." *International Journal of Energy Research* Vol. 43 No. 11 (2019): pp. 5552–5571. DOI 10.1002/er.4529.

[6] Niebuhr, C. M., van Dijk, M., Neary, V. S. and Bhagwan, J. N. "A review of hydrokinetic turbines and enhancement techniques for canal installations: Technology, applicability and potential." *Renewable and Sustainable Energy Reviews* Vol. 113 (2019): p. 109240. DOI 10.1016/j.rser.2019.06.047.

[7] Chiang, Hsiao-Wei D., Lin, Chen-Yin and Hsu, Chih-Neng. "Design and performance study of an ocean current turbine generator." *International Journal of Turbo & Jet-Engines* Vol. 30 No. 3 (2013): pp. 293–302. DOI 10.1515/tjj-2013-0010.

[8] Jiang, Boxi, Amini, Mohammad Reza, Liao, Yingqian, Martins, Joaquim R. R. A. and Sun, Jing. "Control co-design

Copyright © 2023 by ASME

of a hydrokinetic turbine with open-loop optimal control." *International Conference on Offshore Mechanics and Arctic Engineering*. OMAE2022-81006. 2022. Hamburg, Germany. DOI 10.1115/OMAE2022-81006.

[9] Amini, Mohammad Reza, Jiang, Boxi, Liao, Yingqian, Naik, Kartik, Martins, Joaquim R. R. A. and Sun, Jing. "Control co-design of a hydrokinetic turbine: a comparative study of open-loop optimal control and feedback control." *American Control Conference*. 2023. To appear.

[10] Hew, W. R., Saat, F. A. Z. Mohd, Irfan, A. R., Mattokit, E., Rosli, M. A. M., Anuar, F. Shikh, Herawan, S. G. and Syahputra, S. I. A. "Computational fluid dynamics modelling of a hydrokinetic turbine." *AIP Conference Proceedings* Vol. 2347 No. 1 (2021): p. 020195. DOI 10.1063/5.0051477.

[11] Contreras, Leidy T., Lopez, Omar D. and Lain, Santiago. "Computational fluid dynamics modelling and simulation of an inclined horizontal axis hydrokinetic turbine." *Energies* Vol. 11 No. 11 (2018): p. 3151. DOI 10.3390/en11113151.

[12] Bilgen, Onur, Wang, Roger, Cao, Yue, Erol, Nazim and Shan, Xin. "A reconfigurable ducted turbine array concept for renewable flow energy harvesting." *AIAA SCITECH 2022 Forum*. AIAA 2022-2222: pp. 1–17. 2022. AIAA, San Diego, CA. DOI 10.2514/6.2022-2222.

[13] Bayat, Saeid, Lee, Yong Hoon and Allison, James T. "Control co-design of horizontal floating offshore wind turbines using a simplified low order model." *Wind Energy Science Conference*. 2021. Hannover, Germany.

[14] Khan, M. J., Bhuyan, G., Iqbal, M. T. and Quaicoe, J. E. "Hydrokinetic energy conversion systems and assessment of horizontal and vertical axis turbines for river and tidal applications: A technology status review." *Applied Energy* Vol. 86 No. 10 (2009): pp. 1823–1835. DOI 10.1016/j.apenergy.2009.02.017.

[15] Chihaia, Rareş-Andrei, El-Leathey, Lucia-Andreea, Cîrciumaru, Gabriela and Tănase, Nicolae. "Increasing the energy conversion efficiency for shrouded hydrokinetic turbines using experimental analysis on a scale model." *E3S Web of Conferences* Vol. 85 (2019): p. 06004. DOI 10.1051/e3sconf/20198506004.

[16] Taghinezhad, J., Mahmoodi, E. and Masdari, R., M. Alimardani. "Spectral Analyses of an Optimized Ducted Wind Turbine Using Hot-wire Anemometry." *Renewable Energy Research and Applications* Vol. 2 No. 2 (2021): pp. 169–173. DOI 10.22044/rera.2021.10938.1060.

[17] Alaskari, Mustafa, Abdullah, Oday and Majeed, Mahir H. "Analysis of wind turbine using QBlade software." *IOP Conference Series: Materials Science and Engineering* Vol. 518 No. 3 (2019): p. 032020. DOI 10.1088/1757-899X/518/3/032020.

[18] Marten, David, Peukert, Juliane, Pechlivanoglou, Georgios, Nayeri, Christian and Paschereit, Christian. "QBLADE: An open source tool for design and simulation of horizontal and vertical axis wind turbines." *International Journal of Emerging Technology and Advanced Engineering* Vol. 3 No. 3 (2013): pp. 264–269.

[19] Boretti, Alberto. "State-of-the-art of MW-level capacity oceanic current turbines." *Nonlinear Engineering* Vol. 9 No. 1 (2020): pp. 361–369. DOI 10.1515/nleng-2020-0022.

[20] Batten, W. M. J., Bahaj, A. S., Molland, A. F. and Chaplin, J. R. "Experimentally validated numerical method for the hydrodynamic design of horizontal axis tidal turbines." *Ocean Engineering* Vol. 34 No. 7 (2007): pp. 1013–1020. DOI 10.1016/j.oceaneng.2006.04.008.

[21] Hodgkin, Amy, Laizet, Sylvain and Deskos, Georgios. "Numerical investigation of the influence of shear and thermal stratification on the wind turbine tip-vortex stability." *Wind Energy* Vol. 25 No. 7 (2022): pp. 1270–1289. DOI 10.1002/we.2728.

[22] Muratoglu, Abdullah and Yuce, Mehmet. "Performance analysis of hydrokinetic turbine blade sections." *Advances in Renewable Energy* Vol. 2 (2015): pp. 1–10.

[23] Nigam, Suyash, Bansal, Shubham, Nema, Tanmay, Sharma, Vansh and Singh, Raj Kumar. "Design and pitch angle optimisation of horizontal axis hydrokinetic turbine with constant tip speed ratio." *MATEC Web of Conferences* Vol. 95 (2017): p. 06004. DOI 10.1051/matecconf/20179506004.

[24] Hasan, Mehedi, El-Shahat, Adel and Rahman, Mosfequr. "Performance investigation of three combined airfoils bladed small scale horizontal axis wind turbine by BEM and CFD analysis." *Journal of Power and Energy Engineering* Vol. 5 No. 5 (2017): pp. 14–27. DOI 10.4236/jpee.2017.55002.

Copyright © 2023 by ASME